Int. J. High Technology Ceramics **4** (1988) 243–262

10

Tensile Creep of Ceramics: the Development of a Testing Facility

F. A. Kandil & B. F. Dyson

Division of Materials Applications, National Physical Laboratory, Teddington, Middlesex TW11 0LW, UK

1 INTRODUCTION

Structural design with ceramics (as with all materials) requires a reliable database of mechanical properties that allows adequate prediction of component behaviour in service. Currently, the majority of ceramics testing at high temperatures is carried out using bending (flexure) methods to create a tensile mode in a part of the testpiece. In flexure tests, fracture starts at or near the surface under tension (not necessarily at the point of maximum stress) due to propagation of surface or subsurface flaws: the rate of propagation depends on the shape and size of *crack-like* defects and the driving force for propagation. In smooth testpieces it is impossible to control the position or size of the defect that will lead to rupture and the measured fracture strength will depend on the volume-fraction of the component that is subjected to the maximum stress. Consequently, 3- and 4-point bending and tensile tests will, generally, produce apparent strength values in a descending order.

In flexure creep testing, the stress field is statically indeterminate and time-dependent. As a consequence, this test has little to recommend it for procuring creep data for structural design, and indeed for studying deformation and/or fracture mechanisms (see Grathwohl (Paper 3) for a fuller account).

The uniaxial tensile test, on the other hand, offers the advantage of having a uniform and time-independent stress field which *can* be subjected to a much larger volume of the material, thus increasing the probability of failure from the bulk: surface effects are *still* present. Tension is also favoured for

testing ceramic/whisker and fibrous composites. Moreover, it is the only mechanical test that can be applied to fibres. However, uniform tensile stresses can only be obtained with systems with extremely good force alignment: any misalignment in the force acting on the testpiece (including that caused by eccentricities due to poor testpiece manufacture) will introduce bending and reduce the measured strength.

Potential high-temperature industrial applications of engineering ceramics require testing at temperatures normally greater than 1000°C and current interest is focused within the range 1200–1500°C. The classic method of creep testing of metals is to enclose the testpiece grips and, partially, the pull-rods and extensometer inside a suitably large furnace. Although primarily used at temperatures below about 1000°C, this method has been adapted for tensile creep testing of ceramic materials by, amongst others, Gangler (1950), Kossowsky (1974), Birch *et al.* (1978), Govila (1982) and—for tensile testing only—Ohji *et al.* (1987). With this method, henceforth termed the hot-grip (HG) method, the maximum operating temperature is usually restricted by the maximum allowable temperature of the hot parts of the load-train rather than by the material used for the testpiece. For example, Birch *et al.* (1978) had to use a nitrogen atmosphere in order to prevent oxidation of their molybdenum grips and extensometers and the maximum temperature attainable was apparently limited to about 1300°C.

With a few exceptions thermal conductivities of ceramics are lower than those of most high temperature metallic alloys. Furthermore, and unlike metals, they generally decrease as temperatures increase. This low thermal conductivity of ceramics at high temperatures has been utilised by Chang (1959), Davis & Sinha Ray (1971) and Heawood (1984) to overcome the formidable problem of attachment of testpieces by using grips outside the heated zone. This method, henceforth termed the cold-grip (CG) method, can achieve higher test temperatures than the HG method, but requires longer testpieces.

One major problem in some recent tensile testing systems is the lack of assessment of non-axiality of loading, and tests have been considered valid once they sustain the initial full loading without sudden breakage. As a solution, Kossowsky (1974), Govila (1982), Ohji *et al.* (1987) and others used strain gauges attached to the ceramic testpiece in every test. The strain gauges burn off without causing any apparent surface damage (Kossowsky, 1974). Liu & Brinkman (1986) designed a self-aligning grip system for fatigue testing that can reduce bending stresses to a very small value of about 0·5%. However, this system is expensive and may not be suitable for dead-weight creep testing machines. Furthermore, it requires (as with the majority of existing methods) an 'ideally' machined testpiece that can only be manufactured with very tight machining tolerances.

This paper presents a simpler system for high temperature tensile creep testing developed at the National Physical Laboratory. It is based on an initial design by Morrell (1972) and Barry *et al.* (1975) for long-term creep testing of glass ceramics and refractories at temperatures up to 1200°C. For the sake of completeness, the paper includes Morrell's initial design concept but, in addition, reports on further developments found necessary for testing engineering ceramics at much higher temperatures.

2 FORCE-ALIGNMENT IN TENSILE TESTING OF CERAMICS

Causes of stress non-uniformity in tensile testing include: poor alignment of the top and bottom grip centreline; poor conformance of the testpiece centreline to the top and bottom grip centrelines; and asymmetric machining of the testpiece itself. An eccentric elastic load in a cylindrical testpiece will cause a bending stress σ_b according to the formula

$$\frac{\sigma_b}{\sigma_0} = \pm 4e/r \tag{1}$$

where e is the eccentricity, r is the radius and σ_0 is the average tensile stress.

In routine tensile testing of most engineering materials, effects due to non-uniformity of stress will be insignificant if sufficient plastic flow occurs during the test to attenuate the stress concentrations. However, when testing under conditions where plasticity is confined to a small fraction of the testpiece volume (for example, a testpiece containing a notch) or when plastic flow is limited by inherent brittleness of the tested material, a small misalignment may give rise to high bending stresses and can cause noticeable effects on the test results.

Bending stresses, when superimposed on an axial stress, will cause a non-uniform stress distribution across the section; stress values will range from $\sigma_0(1 - B)$ to $\sigma_0(1 + B)$, where B is the bending strain ratio

$$B = \frac{\varepsilon_b}{\varepsilon_0} \tag{2}$$

At room temperature, localised stresses continue to build up because there is no local yielding: a crack forms at one or more points of stress concentration and, finally, spreads rapidly over the section. Consequently, monotonic, cyclic and static fatigue of ceramics at room temperature are phenomena that are most sensitive to effects due to non-uniformity of stress. Stresses, therefore, have to be measured very accurately and, more importantly, must be uniform.

At high temperatures, fracture may be due either to crack growth or creep ductility exhaustion or both, depending upon the material, temperature and stress (Evans, 1985; Evans & Dalgleish, 1987). If the temperature is sufficiently high and the stress is suitably low, then local, and sometimes general yielding can take place and attenuate initial bending stresses. In situations where both crack growth and creep can take place, non-uniformity of stress is likely to favour crack growth as the dominant fracture mechanism.

The effect of the value of B on scatter of tensile stress-rupture data will depend upon the stress exponent in Norton's Law ($\dot{\varepsilon}_{ss} \propto \sigma^n$, where $\dot{\varepsilon}_{ss}$ is the secondary creep rate). Reported values of B in the literature are between 3 and 5%: these values were measured at room temperature and could have been greater after heating. Until an experimental study of such effects is conducted, we suggest that the maximum allowed value of B for ceramic creep testing should be $\pm 3\%$.

3 MECHANICAL ASPECTS OF THE NATIONAL PHYSICAL LABORATORY (NPL) SYSTEM

The arrangement of the NPL system as designed by Morrell (1972) is shown schematically in Fig. 1. The gauge length of the ceramic testpiece was heated with a small tube furnace; outside this section, the temperature of the testpiece fell steeply. The testpiece was cool enough at its ends to allow the use of an epoxy adhesive to attach it to two metallic end-caps which were further cooled by two water-cooling jackets. This facilitated the design and use of grips and extensometer that were essentially operating at room temperature. The main components of the system and the developments made to facilitate its usage up to 1500°C are described in some detail in the following sections.

3.1 Testpiece-holders and methods of loading

The design principle of the testpiece-holders, shown schematically in Fig. 2, consisted basically of two perpendicular knife-edges brought to bear upon a grooved spacer. One knife-edge was simply-supported by a U-shaped joint, the latter being screwed to a pull-rod. The other knife-edge was assembled into a bracket/sleeve that held the testpiece-cap with a hardened steel pin.

The knife-edges and spacers were constructed of hardened silver steel in the following manner. A cylindrically ground bar was machined at mid-length to create the knife-edge, leaving the ends to act as seats for support. Thus, any rotation of the testpiece axis relative to the loading axis in a plane

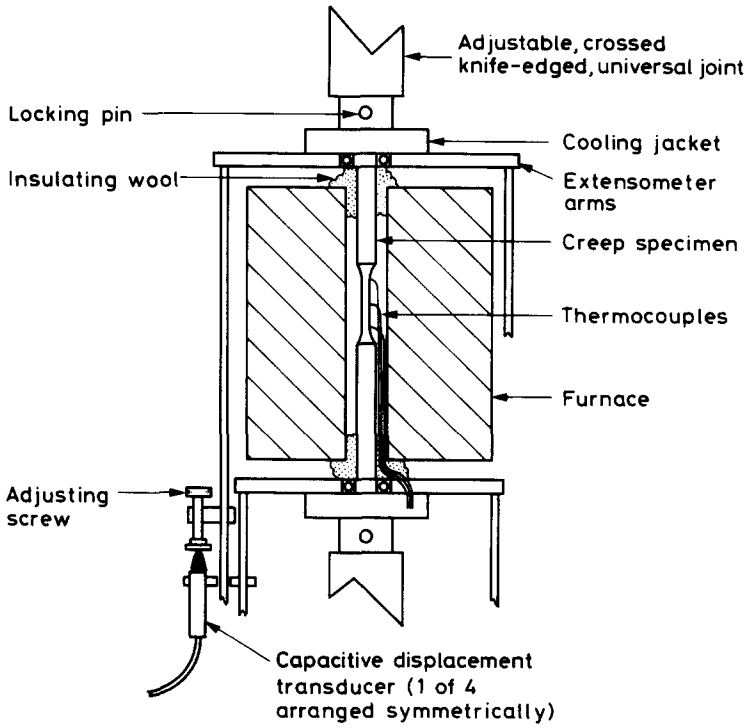

Fig. 1. Schematic drawing of the design concept of the tensile-creep machine.

perpendicular to that of the knife-edge produced no off-axis loading. But a small off-axis loading could be introduced by translating the grooved spacer horizontally in two directions by means of positioning screws: a very fine thread enabled controlled adjustments.

The original design has been modified to enable extra-fine adjustments to be made—the tip of one knife-edge being manufactured eccentrically, as shown in Fig. 2. This makes it possible to obtain very small displacements of the testpiece by rotating the knife-edge about its axis.

It was also possible to adjust the axiality of the system by rotating the whole testpiece-holder assembly about the vertical axis; however, this is not recommended and should only be used for checking the true axiality of the load-train before mounting the ceramic testpiece.

In this manner, the system was able to translate the testpiece to a position where its centreline coincided with the top and bottom centrelines of the load-train. At the same time, the testpiece-holders were self-adjusted in angular directions, thus further reducing bending due to possible bowing of the testpiece when loaded.

The testpiece-holders had a maximum designed capacity of 5 kN.

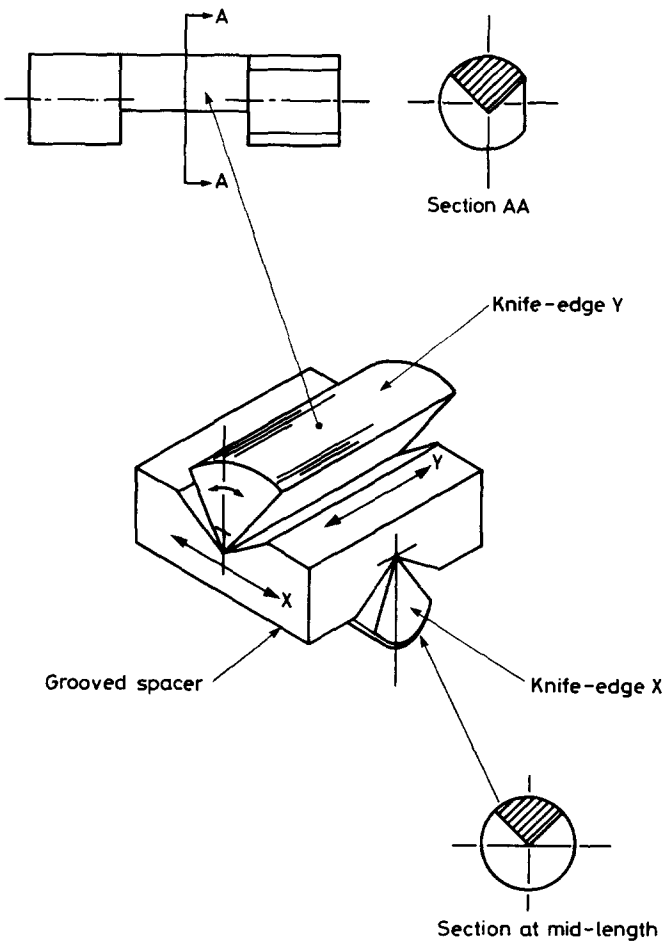

Fig. 2. Schematic for the design principle of the universal joint.

The machine frame was derived from a constant-load creep machine and developed with the possibility of loading the testpiece in one of two ways:

(i) Loads within the range 500 N to 5 kN (or about 40 to 400 MPa stress at the testpiece gauge length) were applied via a single beam having a 10:1 ratio.

(ii) Small loads ranging from 20 to 500 N (about 1·5 to 40 MPa) were better applied by suspending weights directly from the testpiece via a virtually frictionless self-aligning holder. The use of a self-aligning holder limited the ability to realign the testpiece; thus, only testpieces with an eccentricity of 10 μm, or less, could be used with this method of loading.

3.2 Extensometry

The compactness required in the furnace design did not permit extensometers to be attached directly to the testpiece gauge length. The extensometer shown in Fig. 3 consisted of two cruciform beams made of aluminium alloy; the beams, measured between the centrelines of the testpiece and the transducers, were 70 mm long. The beams were clamped on to the testpiece shanks so that their directions coincided exactly with the two planes of the knife-edged joints of the testpiece-holders. Four slender rods, made of Invar 36, were attached to the top beams and slid into clearance holes made through four small aluminium pieces which were

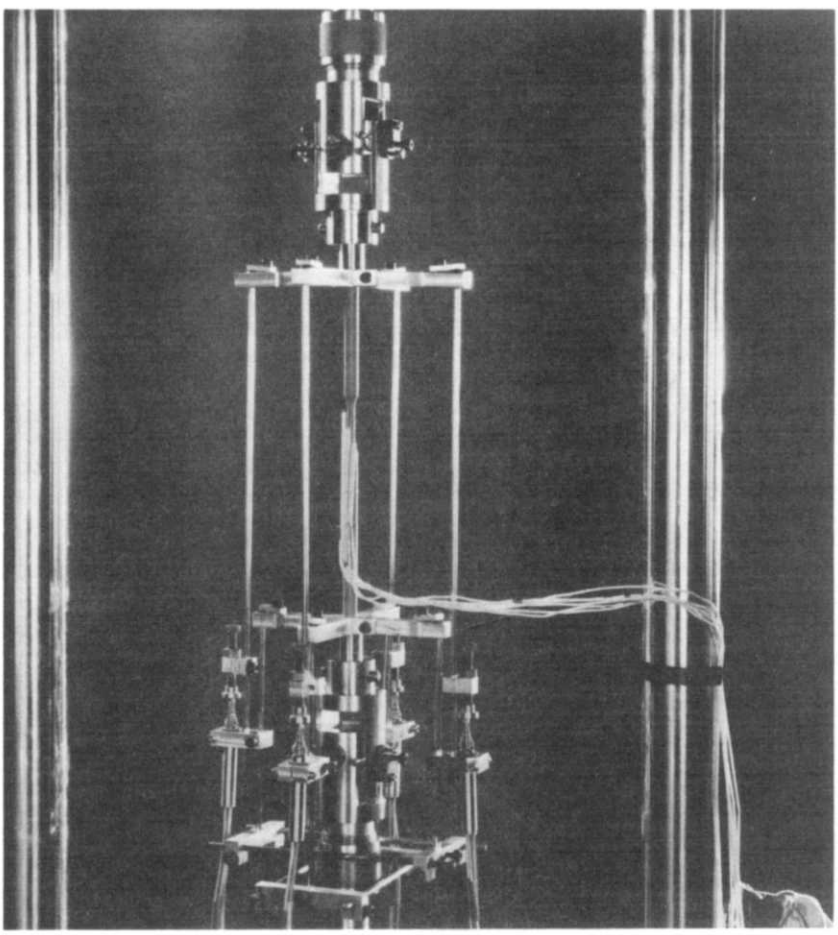

Fig. 3. Close-up view of the extensometer assembly. The furnace has been removed to show the arrangement of the thermocouples on the specimen.

clamped on to the bottom extensometer beams. Extension was measured by four capacitive transducers, which had a resolution of 10 nm.

It is interesting to note that because the extensometer beams acted as cantilevers, the bending measured by the transducers was 35 times the actual value on the gauge length of the testpiece. Thus, the mean axial extension (e_m) is

$$e_m = \frac{e_1 + e_2}{2} \tag{3}$$

and the bending ratio B on the surface of the gauge length of the testpiece is

$$B = \frac{1}{35} \frac{e_1 - e_2}{e_1 + e_2} \tag{4}$$

where e_1 and e_2 are the extensions measured by two transducers operating in one plane.

Two creep curves were obtainable in every test, each creep curve being the average of the readings of the transducers that operated in one plane.

3.3 Furnace and temperature control system

The specially designed furnace had a cylindrical form measuring 165 mm overall height, 115 mm outside-casing diameter and 19·5 mm diameter bore. The furnace had a single-zone winding made of 20% Rh–platinum alloy wire with a hot zone of about 25 mm at a mean temperature of 1500°C, with a uniformity within $\pm 2{\cdot}5$°C.

While increasing the temperature capability of the original system from 1200 to 1500°C, it was found essential to improve the means of control of temperature. A programmer-controller is now connected to one of three type R thermocouples measuring the temperature along the length of the testpiece. Temperature stability was considered to be of prime importance and has been kept within $\pm 0{\cdot}5$°C at all temperature levels. Being designed with a low thermal mass, the furnace could reach 1500°C within 90 min.

3.4 Testpiece design

The testpiece, shown in Fig. 4, was manufactured from a solid cylindrical rod of the ceramic material, 9·4 mm in diameter and 270 mm long. Two metallic caps were glued to the ceramic rod at each end by a strong adhesive. The gauge section was 4 mm in diameter and 22 mm parallel length with a transition radius of 15 mm.

Newly designed end-caps were made of stainless steel with a locating centre pip in one end while the other end was drilled to accept the 9·4 mm

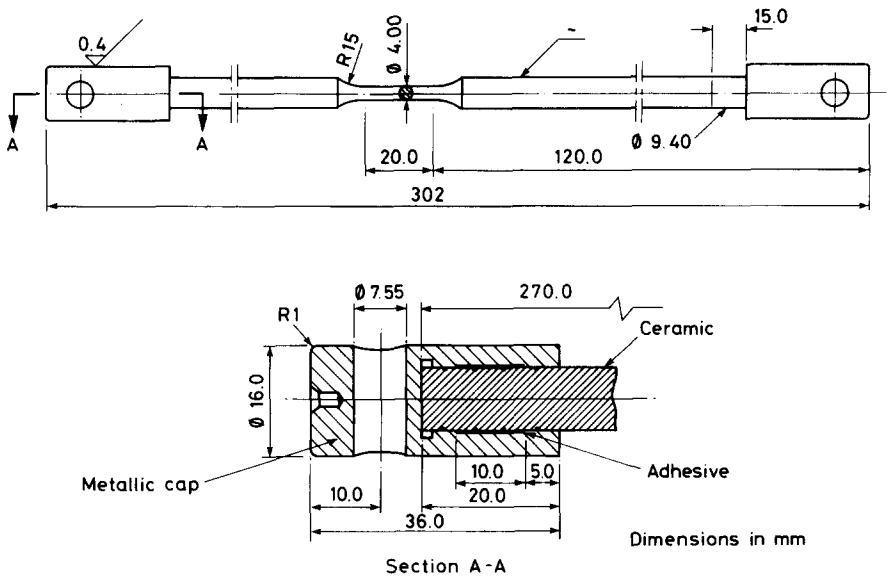

Fig. 4. Details of the ceramic tensile specimen.

ceramic rod with about 10 μm clearance. A single gap, 0·5 mm deep and 10 mm long, was made on the inside of each end-cap in order to accommodate the adhesive; furthermore, shallow circumferential grooves were machined on the ceramic rod to make a stronger grip with the adhesive. The adhesive was a toughened single-part epoxy type, capable of operating at temperatures of up to about 200°C. In order to ensure coaxiality of the caps, each was clamped in a vee-block whilst the adhesive was being cured. Each mounted testpiece was then machined by cylindrical grinding using high-speed, contoured grinding wheels. During this process, the testpiece rotated about the two centres of the end-caps.

Care was taken to ensure: (i) good roundness of the gauge section; (ii) concentricity between the centreline of the testpiece and the outside surfaces of the end-caps. Although the specified limit of eccentricity between the gauge length and the end-caps was 10 μm, the final checks on machined testpieces revealed that eccentricities ranged from 5 to 34 μm: this was easily accommodated by the alignment system.

The gauge length of the testpiece was not positioned midway between the end-caps because of the asymmetric distribution of the temperature profile, the precise location of the gauge length being decided after two temperature-profile calibrations had been determined at 1000 and 1450°C. The result of these tests is given in Fig. 5. It may be noted that the testpiece itself was placed such that the temperatures at the end-caps were almost equal, a value of 60°C being measured when the reduced section was at 1450°C.

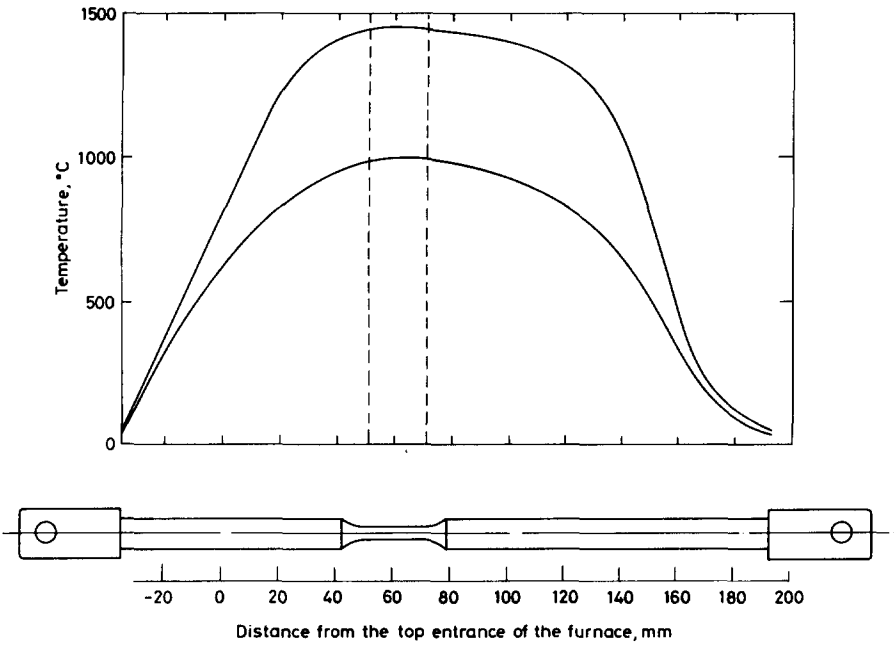

Fig. 5. Temperature-profile calibrations of the test specimen.

4 EXPERIMENTAL ASSESSMENT

To assess the capability and accuracy of various aspects of the system, a series of tests was conducted using testpieces made of reaction-bonded silicon nitride (RBSN). The material was manufactured by Tenmat Ltd and chosen because it retains good creep properties at high temperatures. According to data supplied by the manufacturer, the material had the following properties:

Modulus of rupture	190 MPa
Compressive strength	550 MPa
Young's modulus	170 GPa
Thermal expansion coefficient	$3 \times 10^{-6} K^{-1}$ (300–1300 K)
Thermal conductivity	$16 Wm^{-1}K^{-1}$ (300 K)
Bulk density (NPL measurement)	$2{\cdot}56 gm\ cm^{-3}$
Porosity	about 20%

The assessment of the system comprised, mainly, of the following stages: (i) assessment of the main components on an individual basis; (ii) tensile tests at room temperature; (iii) creep tests at 1450°C.

4.1 Force realignment

The ability of the testpiece-holders to align the tensile force acting upon the cross-section of the testpiece was assessed in the following manner. A 5-mm diameter dummy testpiece made of stainless steel was instrumented with four strain gauges arranged symmetrically around the circumference at the middle of the gauge length. Small loads were applied incrementally to the testpiece and necessary adjustments were made (using the testpiece-holders' positioning screws) to minimise the side-to-side differences of the gauges' readings. An iterative procedure of loading/position-adjustment continued until all four gauges gave identical readings. Repeatability of loading, without removing the testpiece, was within $\pm 2\%$ bending. Afterwards, all the screws were tightened to lock the system and prevent further displacement of the knife-edges.

4.2 Tensile tests at room temperature

After aligning the force transmission system, as described in the preceding section, a ceramic testpiece was mounted in the manner shown in Fig. 3, except that the extensometer was clamped on to the shanks just outside the reduced section. A small load, typically to create an extension of about 1 μm, was applied and the testpiece was realigned to eliminate bending—this time by using the transducers instead of the strain gauges. Iterative adjustments were made until the bending was reduced to about 1–2%. The specimen was then incrementally loaded until fracture occurred.

Since the deformation was purely elastic, the total extension measured by the extensometer (e_m) over a length l is given by:

$$e_m = \int_0^l \frac{P}{AE} \mathrm{d}l \tag{5}$$

where P is the applied load, A is the cross-sectional area and E is Young's modulus.

For the specimen geometry and extensometer arrangement used, and according to the analysis in Appendix 1, the deformation in the gauge length (e_{gl}) is:

$$e_{gl} = 0{\cdot}627\, e_m \tag{6}$$

where e_m is the extension measured by the extensometer. The resulting stress–strain plot, derived from two tests, is presented in Fig. 6. The stress–strain relationship, as expected, was purely elastic with a Young's modulus of 170·8 GPa which is in good agreement with the value given by

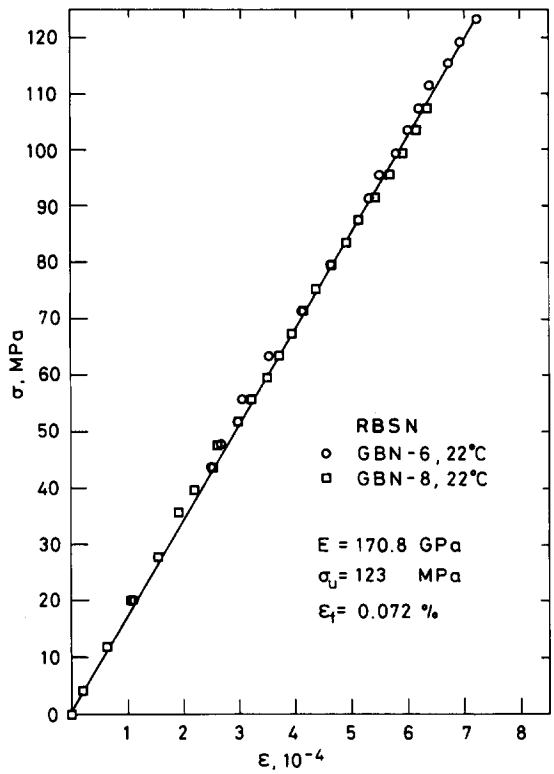

Fig. 6. Tensile stress–strain plot of RBSN at room temperature.

the material manufacturer. The fracture stress and strain-to-rupture were about 123 MPa and 0·072%, respectively.

4.3 Creep tests

Five creep tests were carried out at a test temperature of 1450 ± 2·5°C and a stability within ±0·5°C. The stress levels in these tests were chosen to give times-to-rupture within the range 1–1000 h. As with the tensile tests at room temperature, bending stresses were reduced to within ±2%.

The testing procedure was as follows.

(1) The force transmission system was initially aligned as described in Section 4.1.

(2) Three Pt/Pt13Rh thermocouples, shielded by thin alumina tubes were attached to the specimen shank using platinum alloy wires; the nearest attaching point to the reduced section transition radius edge was about 15 mm away. As shown in Fig. 3, the thermocouples

were made to follow the profile of the gauge length but not physically touch it. The beads were left unshielded to reduce the possibility of contaminating the tested material by either the thermocouple material or sheath. Maximum error in temperature measurement was believed to be less than $\pm 2°C$: see Discussion.

(3) The testpiece, loading-train and extensometer were assembled and a first run was made to realign the loading system.

(4) With Kaowool placed in each end of the furnace for insulation, a second run was made to realign the loading system in order to ensure that the bending stresses were still below 2% (Fig. 7).

(5) With a small load applied (typically 20N, $\sigma = 1{\cdot}5$ MPa), the testpiece was heated at a rate of about 10°C min^{-1}. After reaching the test

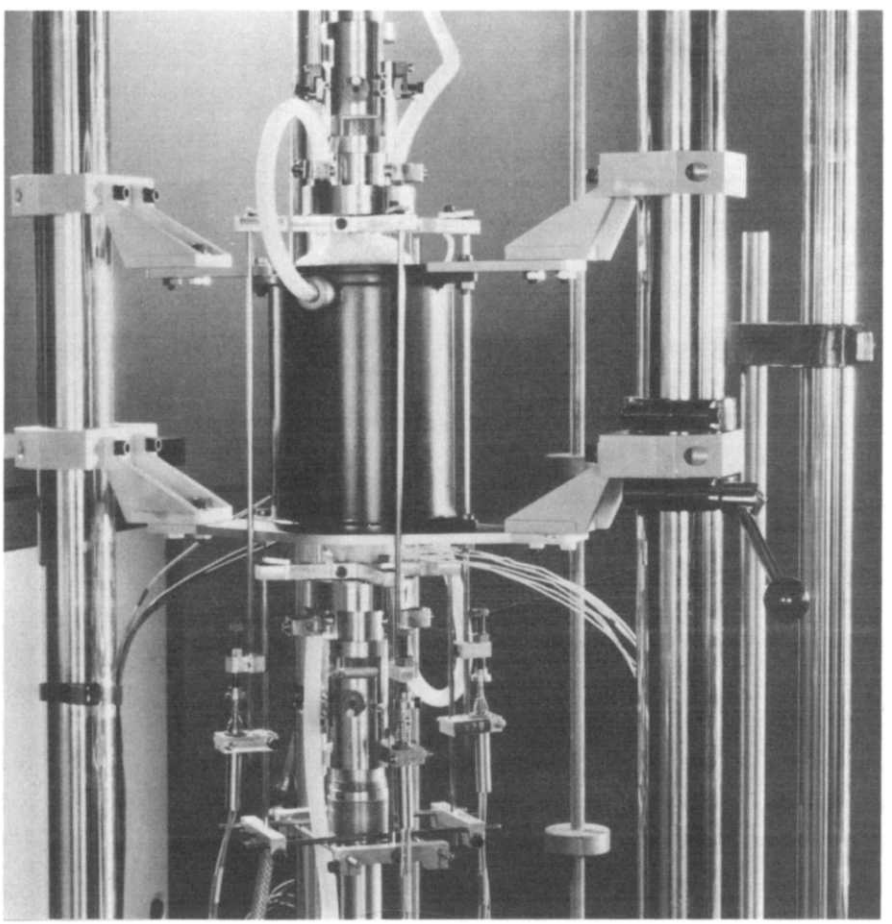

Fig. 7. A close-up showing the furnace, extensometers, cooling jackets, the universal joints and parts of the loading train.

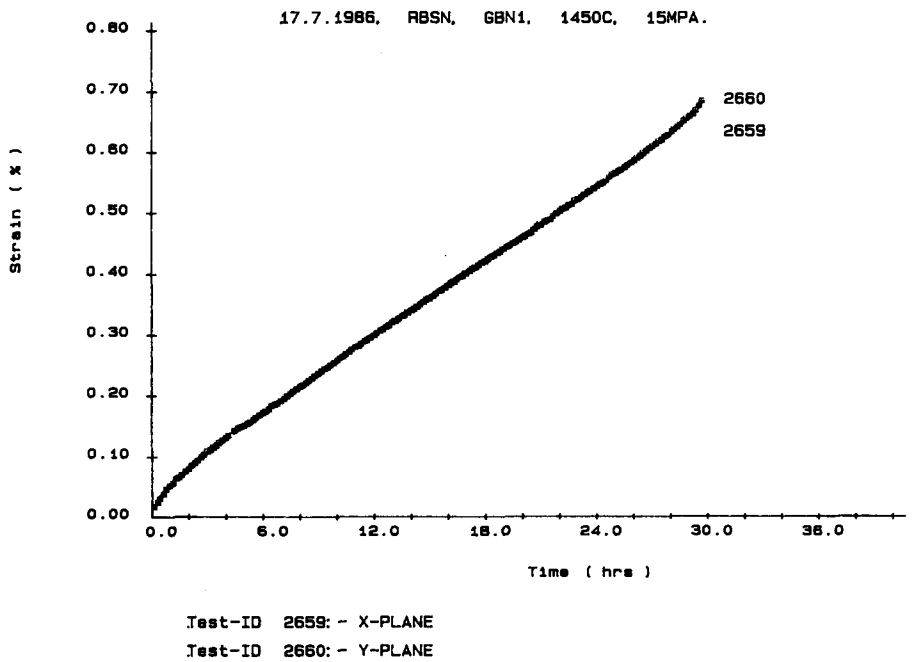

Fig. 8. Two creep curves (one in a particular plane and the other normal to it) of RBSN at 1450°C, 15 MPa.

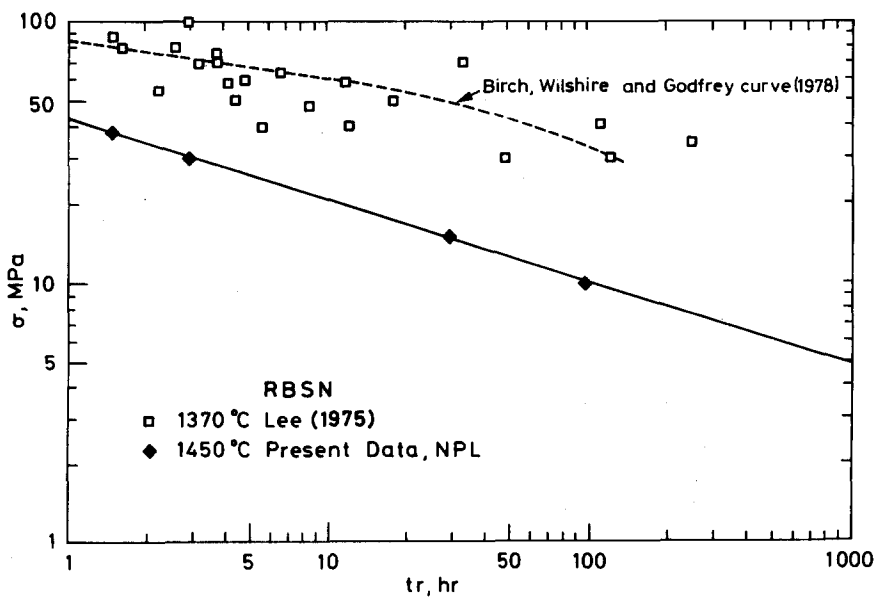

Fig. 9. Stress-rupture data of RBSN at two temperatures. The data at 1370°C were obtained by Lee (1975).

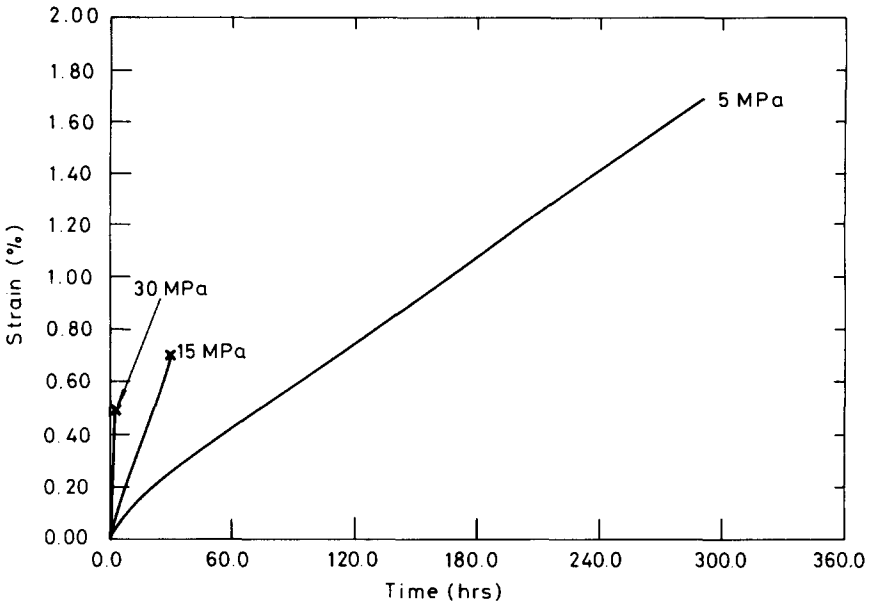

Fig. 10. Creep curves at three stress levels superimposed to show the effect of loading on the rupture strain.

temperature, the testpiece was left for 24 h so that surface oxidation was almost completed.

(6) Before the creep load was added, the system alignment was checked once more. Further adjustments to the universal joints were neither needed nor recommended during the test.

(7) When the testpiece fractured, the furnace switched off automatically.

Figure 8 shows a typical result: as can be seen in the figure, the two creep curves, one for each orthogonal axis, were almost indistinguishable.

The stress rupture data at 1450°C, shown in Fig. 9, can be represented by:

$$t_r = 1{\cdot}7 \times 10^5 \sigma^{-3{\cdot}21} \tag{7}$$

where t_r is the time-to-rupture in hours and σ is the applied stress in MPa. The creep 'ductility' or rupture strain increased as the stress level decreased (Fig. 10).

It is important to mention that the strain indicated in Figs 8 and 10 is the measured extension divided by the effective gauge length of the testpiece which was 21·53 mm: see Discussion. Also, the test conducted at 5 MPa, shown in Fig. 10, was interrupted at the time shown and not fractured.

Other RBSN data obtained at 1370°C by Lee (1975), are also included in Fig. 10. The scatter in NPL's data was $\pm 10\%$ (in time-to-rupture) compared with about $\pm 1000\%$ for the other data.

5 DISCUSSION

The system has been found more able to reduce bending stresses than other methods reviewed by Christ & Swanson (1976), including those using conventional universal joints employing ball bearings (Davis & Sinha Ray, 1971) and powder-cushion gripping (Lange & Diaz, 1978).

The ability of the extensometers to measure bending at low stresses can be demonstrated in the following example. Assuming 1 μm extension and 2% bending, then according to eqns (3) and (4), the transducers' readings would be $e_1 = 1{\cdot}7\ \mu$m and $e_2 = 0{\cdot}3\ \mu$m. With a side-to-side difference of $1{\cdot}4\ \mu$m, these extensions could be measured accurately. In contrast, a conventional type of extensometer, i.e. with limbs attached directly to the specimen's gauge length, would give extension values of 1·02 and $0{\cdot}98\ \mu$m. The difference $(e_1 - e_2)$ in the latter case of only $0{\cdot}04\ \mu$m is too small to be measured accurately with current transducers.

Because the extension measured was the sum of the extensions in the parallel length, the fillets and the shoulders of the testpiece, the strain values were, therefore, subject to some error if they were to be calculated over the 20-mm parallel length. Appendix 2 describes a method of subdividing the measured extension and leads to expressions for the ratio of the measured creep rate $\dot{\varepsilon}_m$, to the creep rate at the centre of the gauge length $\dot{\varepsilon}_0$, of known temperature T_0 (eqns (A11) or (A12)). For the conditions of the present tests, we have substituted the following input parameters into Eqn (A11): $Q = 650\ \text{kJ mol}^{-1}$ (Birch *et al.*, 1978); $n = 1{\cdot}7$; giving $\dot{\varepsilon}_m/\dot{\varepsilon}_0 \simeq 1{\cdot}08$. The ratio $\dot{\varepsilon}_m/\dot{\varepsilon}_0$ was used to derive an effective gauge length as given in Eqn (A13).

Temperature fluctuations inside and outside the furnace were kept very low. The furnace temperature was stable to within $\pm 0{\cdot}5$°C, which caused thermal expansions/contractions of the tested testpiece of about $\pm 0{\cdot}33\ \mu$m. Room temperature was controlled to within ± 1°C, which would cause errors in the measured extension of about $\pm 0{\cdot}18\ \mu$m per degree C: these errors were random and insignificant.

In order to avoid possible contamination, the temperature of the testpiece was measured using thermocouples with unshielded beads, in close proximity to the surface of the testpiece. There are potential errors in the measurement of temperature with this procedure and so an independent calibration was made to determine their magnitude. One thermocouple was placed inside an alumina tube to act as a shield; another with its bead unshielded was attached to the alumina tube so that both beads were at the same height. The composite thermocouple was then inserted into the furnace at a nominal temperature of 1450°C. The unshielded thermocouple indicated a value of temperature 2°C higher than the shielded one. Many more separate tests would have to be performed in order to establish whether this small difference was due to systematic or random errors. For

the present work, it has been assumed that the 2°C is a random error and no corrections have been made in reporting the measured temperature.

Data-scatter is attributed to the characteristics of the material tested *and* the testing technique. Improving the testing method (by ensuring stress and temperature uniformity and the better control of temperature stability) should reduce the experimental scatter and ultimately any data-scatter *will* only be due to material behaviour. The reduction in data-scatter observed in the NPL's data shown in Figs 6 and 9 has been encouraging but more tests are needed to establish the scatter due to inherent material behaviour with more certainty. It is also important to draw the same argument to Lee's data (Fig. 9; Lee, 1975) which showed greater scatter. Since that author did not measure the bending due to off-axiality of loading in his experiments, one cannot quantify how much scatter was due to his testing technique.

6 CONCLUDING REMARKS

This article has presented a testing facility for tensile creep of ceramics. Particular emphasis has been placed upon designing methods to minimise bending stresses and ensuring good temperature control in order to reduce scatter in the creep data.

The use of knife-edge universal joints minimises frictional effects, and allows low-stress tests to be performed. It has been demonstrated that the extensometer is superior to the conventional type for measuring bending strains. The error in strain due to measuring the extension outside the furnace can be estimated and is small compared to potential errors associated with the measurement of the absolute value of temperature.

The system is able to perform tests up to 1500°C in air with a bending stress below 2% of the applied tensile stress. To achieve this, the force-transmission system does not require a 'perfectly' concentric testpiece.

The experimental assessment, using RBSN testpieces at room temperature and 1450°C has confirmed the ability of the system to produce consistent results; thus, reliable information can be obtained from fewer tests.

Design optimisation and modifications of the present system are currently being implemented in order to use shorter specimens (150 mm long) and to achieve a higher temperature (1600°C).

ACKNOWLEDGEMENTS

We wish to thank Dr R. Morrell for advice and stimulating discussions. The assistance of Mr R. Peskett in the experimental program and Mr D. Dawson

for performing the ultrasonic measurements is gratefully appreciated. The material was supplied by AE Developments Ltd (now Tenmat Ltd).

REFERENCES

Barry, T. I., Lay, L. A. & Morrell, R. (1975). High temperature mechanical properties of condierite refractory glass ceramics. *Proc. Brit. Ceram. Soc.*, **25**, 67–84.

Birch, J. M., Wilshire, B. & Godfrey, D. J. (1978). Deformation and fracture processes during creep of reaction bonded and hot pressed silicon nitride. *Proc. Brit. Ceram. Soc.*, **26**, 141–54.

Chang, R. (1959). High temperature creep and anelastic phenomena in polycrystalline refractory oxides. *J. Nucl. Mater.*, **2**, 174–81.

Christ, B. W. & Swanson, S. R. (1976) Alignment problems in tensile testing, *J. Test. and Eval.*, **4**(6), 407–17.

Davis, C. K. L. & Sinha Ray, S. K. (1971). A simple apparatus for carrying out tensile creep tests on brittle materials up to temperatures of 1750°C, *J. Phys. E.: Sci. Instrum.*, **4**, 421–4.

Evans, A. G. (1985). Engineering property requirements for high performance ceramics, *Mater. Sci. Engng*, **71**, 3–21.

Evans, A. G. & Dalgleish, B. J. (1987). Some aspects of the high temperature performance of ceramics and ceramic composites. In *Creep and Fracture of Engineering Materials and Structures*, ed. B. Wilshire & R. W. Evans, Inst. of Metals, London, pp. 929–55.

Gangler, J. J. (1950). Some physical properties of eight refractory oxides and carbides, *J. Am. Ceram. Soc.*, **33**(12), 367–74.

Govila, R. K. (1982). Uniaxial tensile and flexural stress rupture strength of hot-presssed Si_3N_4, *J. Am. Ceram. Soc.*, **65**(1), 15–21.

Heawood, C. M. (1984). *Tensile creep testing of ceramics development of a testing facility*. Admirality Marine Technology Establishment, Holton Heath, Dorset, UK, ARE HH TM 84215.

Kossowsky, R. (1974). Creep and fatigue of Si_3N_4 as related to microstructures. In *Ceramics for High-Performance Applications*, ed. J. J. Burke, A. E. Gorum & R. N. Katz, Proc. 2nd Army Material Technology Conf., 13–16 Nov. 1973, Hyannis, Massachusetts, pp. 347–71.

Lange, F. F. & Diaz, E. S. (1978). Powder-cushion gripping to promote good alignment in tensile testing, *J. Test. and Eval.*, **6**(5), 320–3.

Lee, J. M. (1975). *The tensile stress testing of reaction bonded silicon nitride*, Admiralty Materials Laboratory, Holton Heath, Dorset, UK, Memo. MC 275/75.

Liu, K. C. & Brinkman, C. R. (1986). Tensile cyclic fatigue of structural ceramics. In *Proc. 23rd Automotive Technology Development Contractors' Coordination Meeting*, held at Dearborn, Mi., October 1985. Society of Automotive Engineers Inc., Warrendale, Pa., pp. 279–84.

Morrell, R. (1972). A tensile creep-testing apparatus for ceramic materials using simple knife-edge universal joints, *J. Phys. E.: Sci. Instrum.*, **5**, 465–7.

Ohji, T., Sakai, S., Ito, M., Yamauchi, Y., Kanematsu, W. & Ito, S. (1987). Yielding phenomena of hot-pressed Si_3N_4, *High Temp. Technol.*, **5**(3), 139–44.

APPENDIX 1: ESTIMATION OF TIME-INDEPENDENT STRAIN AT THE PARALLEL LENGTH OF THE TESTPIECE

Room temperature testing of monolithic ceramics is typically elastic up to the incidence of fracture: i.e. the strain is proportional to the stress.

The following dimensions of the testpiece are:

parallel length $= 2l_0$,
radius of the gauge section $= r_0$,
axial length of the transition-section $= l_1$,
fillet radius $= r_f$,
length of the shank between the transition-section and the centre of the extensometer limb $= l_2$,
shank's radius $= r_2$,
total distance between the extensometer's limbs $= L$.

For a symmetric extensometer arrangement:

$$L = 2l_0 + 2l_1 + 2l_2 \tag{A1}$$

and the total extension measured by the extensometer, e_m, is

$$e_m = 2e_0 + 2e_1 + 2e_2 \tag{A2}$$

where $2e_0$, $2e_1$ and $2e_2$ are, respectively, the extensions in the parallel length, the transition sections and the shanks of the testpiece. These extensions may be expressed as follows

$$e_0 = \frac{P}{\pi E}\frac{l_0}{r_0^2} \tag{A3}$$

where P is the axial force,

$$e_1 = \frac{P}{\pi E}\int_0^{l_1} [r_0 + r_f\sqrt{(r_f^2 - l^2)}]^{-2}\,dl \tag{A4}$$

$$e_2 = \frac{P}{\pi E}\frac{l_2}{r_2^2} \tag{A5}$$

Equation (A4) may be solved numerically by applying Simpson's integral formula. Substituting eqns (A3)–(A5) into eqn (A2) leads to the evaluation of the constant C in the relationship

$$2e_0 = Ce_m \tag{A6}$$

APPENDIX 2: ESTIMATION OF AN EFFECTIVE GAUGE LENGTH OF THE TESTPIECE FOR CREEP DEFORMATION

Following an analysis similar to the one used by Morrell (1972), we consider a testpiece with a parallel length $2l_0$. Creep occurs over lengths l_1 and $-l_2$, measured from the centre of the gauge length, and beyond which creep can be considered negligible. The strain rate measured by the extensometer ($\dot{\varepsilon}_m$) is:

$$\dot{\varepsilon}_m = \frac{1}{2l_0}\int_{-l_2}^{l_1} \dot{\varepsilon}\,dl \tag{A7}$$

and the strain $\varepsilon_m = \int_0^t \dot{\varepsilon}_m\,dt$ (A8)

The strain rate at a location l is a function of the stress $\sigma(l)$ and temperature $T(l)$, viz.

$$\dot{\varepsilon}(l) = f(\sigma_0, T_0, l) \tag{A9}$$

The sub-symbol (0) denotes the values at the middle of the gauge section.

Consider a creep equation of the form

$$\dot{\varepsilon}(l) = \dot{\varepsilon}_0\left[\frac{\sigma(l)}{\sigma_0}\right]^n \exp\left[\frac{-Q}{RT(l)}\right] \tag{A10}$$

where Q is the activation energy and R is the gas constant.

Substituting of eqn (A10) into eqn (A7) gives:

$$\frac{\dot{\varepsilon}_m}{\dot{\varepsilon}_0} = \frac{1}{2l_0}\int_{-l_2}^{l_1}\left[\frac{\sigma(l)}{\sigma_0}\right]^n \exp\left[\frac{-Q}{RT(l)}\right]dl \tag{A11}$$

For an individual furnace, and a standard testpiece, eqn (A11) shows that the ratio of the measured to true strain rate at the centre of the gauge length is independent of the applied load and a function only of the test temperature (T_0). Equation (A11) may be solved numerically by assuming a small increment of length Δl at a distance l. The increment is subjected to a uniform stress (σ_l) at a temperature $T(l)$, the latter is determined from temperature-profile calibration tests as in Fig. 5.

An approximate solution of eqn (A11) may be expressed as follows:

$$\frac{\dot{\varepsilon}_m}{\dot{\varepsilon}_0} = \frac{1}{2l_0}\sum_{l=-l_2}^{l=l_1}\left(\frac{r_0}{r(l)}\right)^{2n}\exp\left[\frac{-Q}{RT_0}\left(\frac{T_0}{T(l)}-1\right)\right] \tag{A12}$$

Consequently, an effective gauge length of the testpieces may be given as:

$$(2l_0)_{eff} = 2l_0\left(\frac{\dot{\varepsilon}_m}{\dot{\varepsilon}_0}\right) \tag{A13}$$